World Academy of Science, Engineering and Technology
International Journal of Aerospace and Mechanical Engineering
Vol:18, No:3, 2024

Development of an Artificial Ear for Bone-Conducted Objective Occlusion Measurement

Yu Luan

***Abstract*—**The bone-conducted objective occlusion effect (OE) is characterized by a discomforting sensation of fullness experienced in an occluded ear. This phenomenon arises from various external stimuli, such as human speech, chewing, and walking, which generate vibrations transmitted through the body to the ear canal walls. The bone-conducted OE occurs due to the pressure build-up inside the occluded ear caused by sound radiating into the ear canal cavity from its walls. In the hearing aid industry, artificial ears are utilized as a tool for developing hearing aids. However, the currently available commercial artificial ears primarily focus on pure acoustics measurements, neglecting the bone-conducted vibration aspect. This research endeavors to develop an artificial ear specifically designed for bone-conducted occlusion measurements. Finite Element Analysis (FEA) modeling has been employed to gain insights into the behavior of the artificial ear.

***Keywords*—**Artificial ear, bone conducted vibration, occlusion measurement, Finite Element Modeling.

I. Introduction

THE paper focuses on improving an existing artificial ear introduced by Luan et al. [1] during the 24th International Congress on Acoustics. The authors successfully converted the 2D axi-symmetric model of an artificial ear, initially developed by Brummund et al. [2] and improved by Carillo et al. [3], into a 3D prototype for bone-conducted occlusion evaluation.

The challenge in converting a 2D axi-symmetric model to a 3D physical prototype lies in the excitation process. In the 2D axi-symmetric model, excitation involves a force applied from the outer boundary, pushing the ear canal in all directions around the cylinder. However, in 3D prototype, fulfilling this request proves challenging. To address this, the authors [1], [2] directed the excitation unidirectionally. This approach is deemed acceptable since bone-conducted sound/vibration in real life does not occur from all directions. Despite this advancement, the model has room for improvement. One concern pertains to the microphone at the tympanic membrane (TM), which provides different compliance than real TM. Additionally, the 3D model introduces extra resonances than the 2D axi-symmetric model. It influences the sound pressure at TM.

The discussion on the artificial ear is centered around its application in hearing aid industry. The artificial ear is anticipated to be used for validating the behavior of hearing aids concerning OE-related topics, such as occlusion cancelation. Ensuring that the artificial ear closely mimics the human ear is of paramount importance.

Yu Luan is with GN Hearing, Denmark (e-mail: yuluan@gnresound.com).

II. Discussion on the Artificial Ear

A. TM Compliance

The TM compliance plays a crucial role in the occluded ear canal. The bone conducted OE is calculated by dividing the sound in occluded ear canal by the sound in open ear canal. The TM compliance does not significantly impact the sound pressure in the open ear canal, it exerts a substantial influence on the occluded sound.

In open ear canal (EC), the sound pressure at TM contributed by bone conducted vibration is dominated by the acoustic mass of the open EC cavity and the acoustic mass of the radiation of the EC opening. The TM compliance is neglectable in this case.

In the occluded ear canal, the sound pressure at TM is calculated as the product of the acoustic impedance of the occluded EC cavity and the volume velocity imposed by the free EC wall and the medial EP surface. The sound pressure at TM can be approximated in the low frequency range to be [3]-[5]:

$$\hat{p}_{TM}^{occl} = \frac{\hat{q}_{wall}^{occl} + \hat{q}_{EP}}{j\omega(C_{EC}^{occl} + C_{TM})}, \quad (1)$$

where $\hat{q}_{wall}^{occl}$ is the volume velocity of the occluded ear canal walls, $\hat{q}_{EP}$ is the volume velocity of the ear plug's medial surface, C_{EC}^{occl} represents the acoustic compliance of the occluded EC cavity, and C_{TM} represents the TM compliance.

The two compliances in the denominator are of the same order of magnitude. Therefore, having the correct value of the TM compliance in the artificial ear is crucial.

B. Resonances

The artificial ear contains of various parts, each contributes to resonances that result in peaks in the sound pressure response at TM. While some of these peaks disappear in the OE response, others persist.

The OE response is calculated to be [3]:

$$OE = 20\,log_{10}\left(\left|\frac{\hat{p}_{TM}^{occl}}{\hat{p}_{TM}^{open}}\right|\right), \quad (2)$$

where $\hat{p}_{TM}^{open}$ is the sound pressure at TM in the open case. In this context, the OE is purely bone-conducted, representing only to the structure-conducted signal. The sound translated from outside to the ear canal is not considered in this case.

When resonances contribute equal sound pressure at TM in both open and occluded case, these resonances are not manifest

in the OE response. When the contributions are not equalized, the corresponding sound pressure response can be seen.

III. Validating the Artificial Ear by Finite Element Simulations

The artificial ear undergoes validation through finite element simulations using Comsol models designed to replicate the reference model [1].

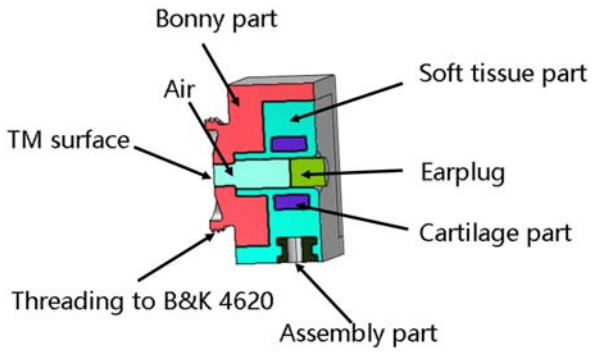

Fig. 1 The artificial ear

The components of the artificial ear are depicted in Fig. 1, with only half of the model displayed. Two modifications are introduced to the original model:

1. An assembly part is added to the bottom, enabling the model to be securely attached to the B&K 4810 shaker.
2. TM compliance is applied to the end of ear canal and compared to the model with acoustic rigid boundary on the same surface. This modification aligns with the physical prototype, which can be presented by introducing the B&K Type 4620 ear simulator. This simulator forms the basis of a new standard ear simulator type 4.3 and provides a unique capability for accurate human ear impedance loading up to 20 kHz.[6]

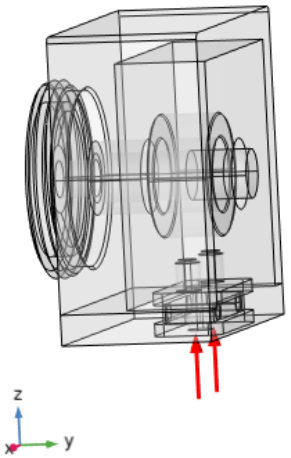

Fig. 2 A unit force is applied to the assembly part; the threading on the prototype serves to attach the B&K type 4620 ear simulator

The model is simulated in both open and occluded case. A unit force is applied to the assembly part at the bottom in the z-direction, as depicted in Fig. 2. Sound pressure at TM is obtained in both open and occluded models. The simulation includes the air inside the ear canal excluding outside air, as the focus is solely on the bone-conducted signals. In the open case, acoustic radiation impedance is applied to the outer surface of the air domain in the ear canal. Conversely, in the occluded case, the ear canal is blocked by a soft foam earplug.

A. TM Compliance

A TM compliance is applied to the artificial ear at the ear canal terminal surface, and the results are compared between models with and without TM compliance.

The difference in sound pressure at the TM are compared between two models: 1. TM compliance applied. 2. TM acoustically rigid. The differences are plotted for models with different insertion depth of the ear plug, as shown in Fig. 3. The plot indicates that larger differences are observed with deeper insertion depth. This observation aligns with (1) that C_{EC}^{occl} becomes smaller with deeper insertion depth, causing C_{TM} to be relatively larger. Consequently, at deeper insertion depth, the presence or absence of TM compliance results in more significant changes in the sound pressure.

The OE exhibits similar behavior as sound pressure, as illustrated in Fig. 4. This similarity is anticipated because the TM compliance is neglectable in the open case. Therefore, the denominator in (2) experiences almost no change, with the numerator dominating the expression.

B. Resonances

Sound pressure at TM is highly influenced by the structural resonances in the artificial ear. The models with TM compliance applied are used for further study on the resonances.

The sound pressure at TM is plotted in an open case and three occluded cases with different insertion depth of the EP: 2 mm, 12 mm, and 20 mm, representing shallow, medium, and deep insertion, respectively (see Fig. 5). The plot reveals similar peak frequencies in open and occluded scenarios. The model patterns are depicted on the main peaks, with the first peak representing a mode in the bottom assembly part, the second peaks related to the fundamental mode in the soft tissue, the third peak corresponding to a mode on the cartilage, the fourth peak elicited by the 2nd mode in soft tissue, and the fifth peaks associated with the 3rd mode in the soft tissue.

The sound pressure at TM results from the combined contributions of two components: EC contribution and EP contribution. In the 2D axi-symmetric model, both EC and EP consistently contribute the same sign of sound pressure [3]. However, in the 3D model, structural resonances introduce a significant phase shift. Each resonance mentioned in Fig. 5 results in a phase shift of π. Additionally, there are resonances not apparent in the total sound pressure response but visible in the individual plot of the EC and EP-contributed sound pressure responses.

Since these resonances belong individually to either EC or EP, the corresponding phase change are unique. Therefore, the two signals are not always in phase. Fig. 6 illustrates the sound

pressure response contributed by EC and EP, respectively, for three different insertions depth. The lower subfigures depict the phase plot of each case, revealing individual resonance from the EC and EP.

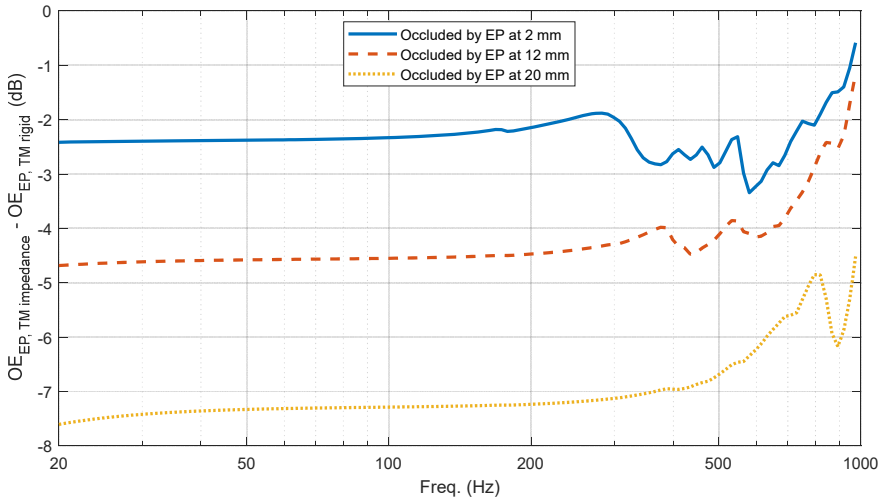

Fig. 4 OE difference with/without TM compliance

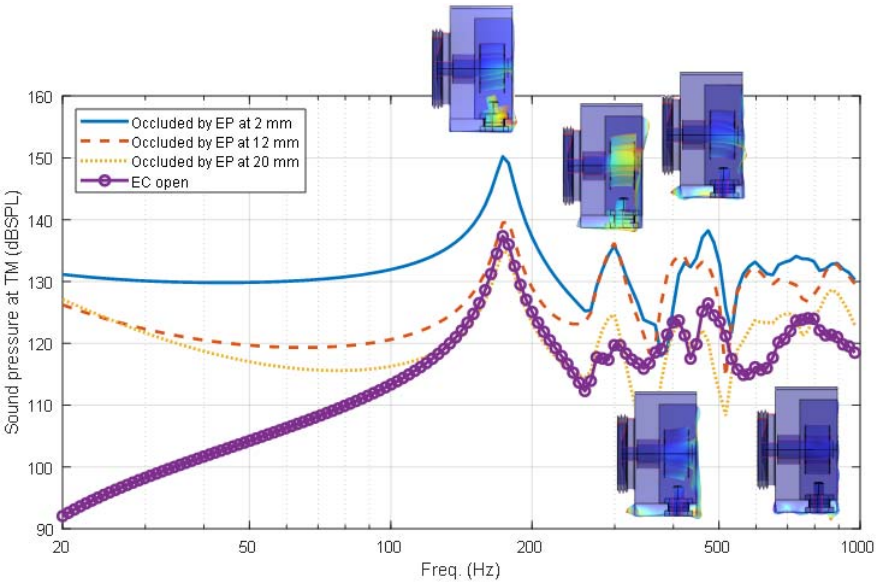

Fig. 5 Sound pressure response at TM and the mode patterns related to the peaks

As observed in the subfigures (a) and (b) of Fig. 6, at shallow insertion (2 mm), the resonance in EP at 27 Hz causes a phase shift of π, resulting in a phase difference between the two signals up to 200 Hz. During this period, the two signals cancel each other, but the amplitude of EP signal is more than 15 dB lower than the EC signal, making the cancellation neglectable.

In the subfigures (b) and (e), as the insertion depth increases to 12 mm, a new resonance in the EC appears at low frequency of 30 Hz. This resonance shifts the phase of EC signal by π, leading to phase coincidence between the two signals up to 200 Hz, as there is no phase change in the EP signal in this range.

The amplitude of the two signals shifts with changes in insertion depth. At 2 mm (shallow insertion), the EC-contributed sound pressure dominates. At 12 mm (medium insertion), the two signals are almost identical, and at 20 mm (deep insertion), the EP-contributed sound pressure dominates. The EP-contributed sound pressure does not vary significantly across insertion depths; the main change is in the EC-contributed sound pressure. It is high at shallow insertion and decreases at deeper insertion due to the smaller radiation area of EC when blocked at deeper insertion.

The OE response is determined by dividing the sound pressure in occluded case by that in the open case. The OE varies with different insertion depth, and a lower OE is anticipated at deeper insertion depths. However, at 20 mm, there is an increased low-frequency response in the OE. As shown in Fig. 6, the EP-contributed signal is prominent and dominates the sound pressure at low frequencies, even though the EC-contributed signal is low. In this case, the EP undergoes significant vibrations, driven by the soft tissue, even though its

inner end is situated within the bonny part of the EC. Furthermore, the OE at the resonances does not exhibit the expected decrease with insertion depth, suggesting that the local deformations in the artificial ear at the resonances are non-linear.

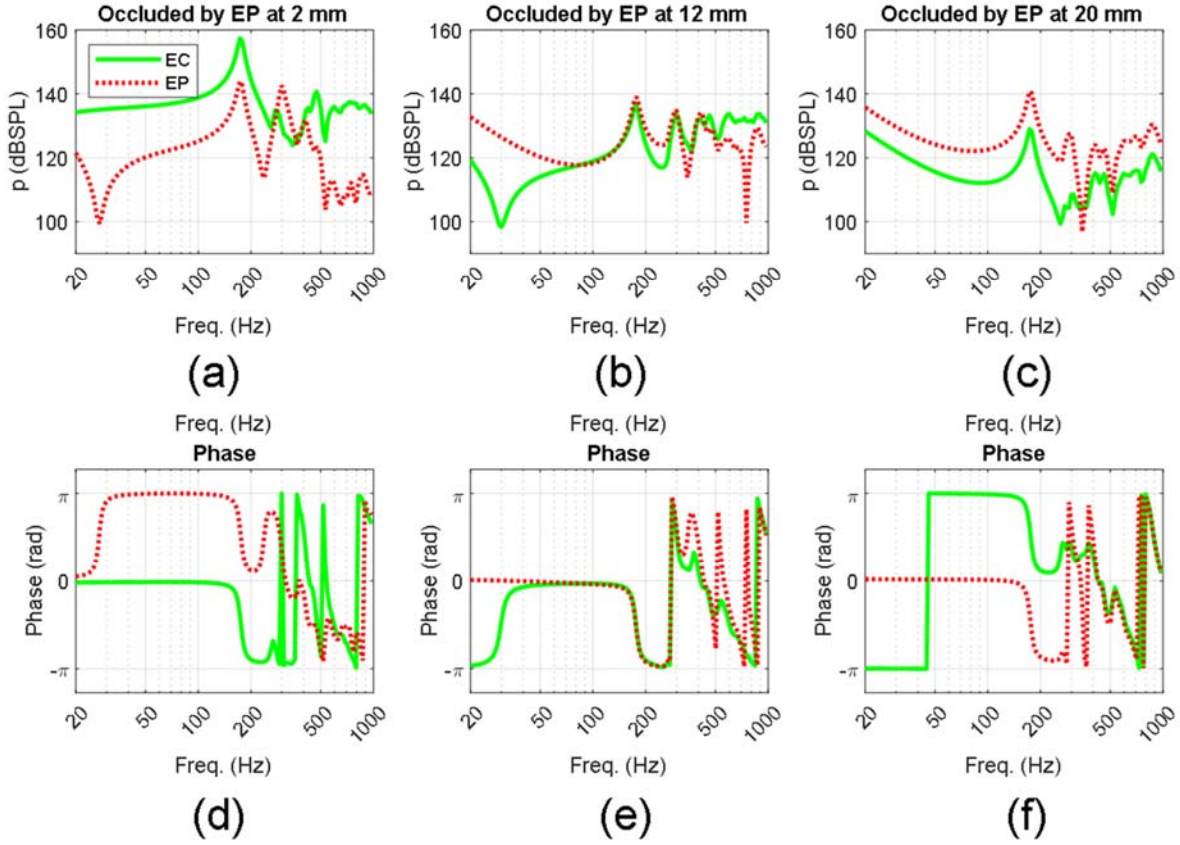

Fig. 6 Sound pressure response at TM contributed by EC and EP

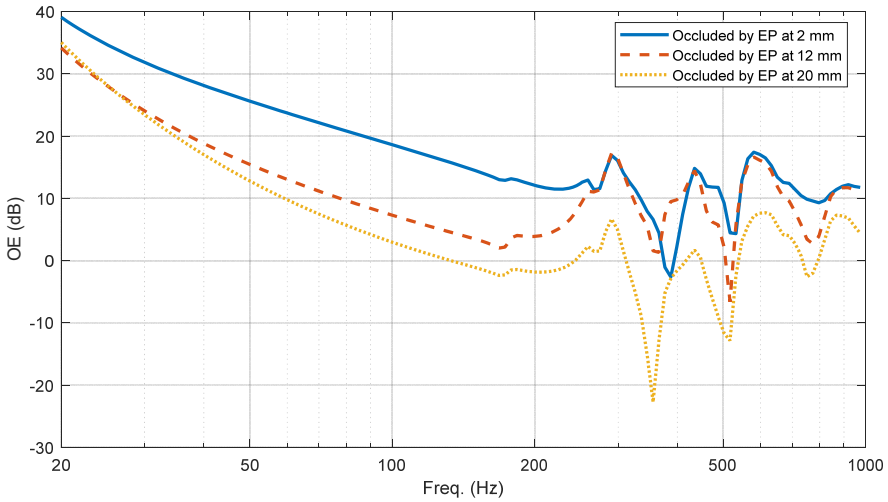

Fig. 7 OE response at different insertion depth

IV. Conclusion

The research presented in this paper contributes to the development and validation of an artificial ear designed specifically for bone-conducted occlusion measurements. The model's accuracy has been improved by modifying the acoustic impedance at the end of the ear canal to match that of the TM. However, the model's downside primarily lies in its resonances, which contribute to extra volume velocities from both the ear canal walls and the ear plug surface. While the model is valid for basic studies, there is room for improvement.

REFERENCES

[1] Y. Luan, M. O. Cyr-Desroches, K. Carillo, O. Doutres, and F. Sgard, "Development and evaluation of an artificial ear for quantifying the objective occlusion effect," 24th International Congress on Acoustics, 2022.

[2] M. Brummund, F. Sgard, Y. Petit, F. Laville, and H. Nelisse, "An Axisymmetric Finite Element Model to Study the Earplug Contribution to the Bone Conduction Occlusion Effect," Acta Acustica united with Acustica, vol. 101, Aug. 2015, doi: 10.3813/AAA.918872.

[3] K. Carillo, O. Doutres, and F. Sgard, "Numerical investigation of the earplug contribution to the low-frequency objective occlusion effect induced by bone-conducted stimulation," J Acoust Soc Am, vol. 150, no. 3, pp. 2006–2023, Sep. 2021, doi: 10.1121/10.0006209.

[4] K. Carillo, O. Doutres, and F. Sgard, "Theoretical investigation of the low frequency fundamental mechanism of the objective occlusion effect induced by bone-conducted stimulation," J Acoust Soc Am, vol. 147, no. 5, pp. 3476–3489, May 2020, doi: 10.1121/10.0001237.

[5] K. Carillo, O. Doutres, and F. Sgard, "Numerical investigation of the fundamental low frequency mechanisms of the objective occlusion effect: focus on the earcanal wall vibration," 2019.

[6] S. Hajarolasvadi, B. Essink, P. F. Hoffmann, A. Ng, U. Skov, and others, "Digital Twin of a Head and Torso Simulator: Validation of Far-Field Head-Related Transfer Functions with Measurements," in Audio Engineering Society Conference: AES 2022 International Audio for Virtual and Augmented Reality Conference, 2022.